crops

MDPI

Article

GWAS for Stripe Rust Resistance in Wild Emmer Wheat (*Triticum dicoccoides*) Population: Obstacles and Solutions

May Tene [1], Elina Adhikari [2,3], Nicolas Cobo [4,5], Katherine W. Jordan [2,6], Oadi Matny [7], Isabel Alicia del Blanco [4], Jonathan Roter [1], Smadar Ezrati [1], Liubov Govta [8], Jacob Manisterski [1], Pnina Ben Yehuda [1], Xianming Chen [9,10], Brian Steffenson [7], Eduard Akhunov [2] and Hanan Sela [1,8,*]

1 Institute for Cereal Crops Research, Tel Aviv University, Tel Aviv 6139001, Israel; tene.may@gmail.com (M.T.); yoniroter@gmail.com (J.R.); ezrati@tauex.tau.ac.il (S.E.); jacobm@post.tau.ac.il (J.M.); pninaby@tauex.tau.ac.il (P.B.Y.)
2 Department of Plant Pathology, Kansas State University, Manhattan, KS 66502, USA; elina1@ksu.edu (E.A.); katherine.jordan@usda.gov (K.W.J.); eakhunov@ksu.edu (E.A.)
3 Department of Horticulture, University of Wisconsin, Madison, WI 54235, USA
4 Department of Plant Sciences, UC Davis, Davis, CA 95616, USA; nicolas.cobo@ufrontera.cl (N.C.); iadelblanco@ucdavis.edu (I.A.d.B.)
5 Departamento de Producción Agropecuaria, Universidad de La Frontera, Temuco 4811230, Chile
6 USDA-ARS, Hard Winter Wheat Genetics Research Unit, Manhattan, KS 66506, USA
7 Department of Plant Pathology, University of Minnesota, St. Paul, MN 55108, USA; onmatny@umn.edu (O.M.); bsteffen@umn.edu (B.S.)
8 Institute of Evolution, University of Haifa, Haifa 3498838, Israel; liubov@evo.haifa.ac.il
9 US Department of Agriculture Agricultural Research Service, Pullman, WA 99164, USA; xianming@wsu.edu
10 Department of Plant Pathology, Washington State University, Pullman, WA 99164, USA
* Correspondence: hans@evo.haifa.ac.il

Citation: Tene, M.; Adhikari, E.; Cobo, N.; Jordan, K.W.; Matny, O.; del Blanco, I.A.; Roter, J.; Ezrati, S.; Govta, L.; Manisterski, J.; et al. GWAS for Stripe Rust Resistance in Wild Emmer Wheat (*Triticum dicoccoides*) Population: Obstacles and Solutions. *Crops* **2022**, *2*, 42–61. https://doi.org/10.3390/crops2010005

Academic Editor: Il-Ryong Choi

Received: 30 December 2021
Accepted: 25 February 2022
Published: 2 March 2022

Abstract: Stripe rust is a devastating disease in wheat that causes substantial yield loss around the world. The most effective strategy for mitigating yield loss is to develop resistant cultivars. The wild relatives of wheat are good sources of resistance to fungal pathogens. Here, we used a genome-wide association study (GWAS) to identify loci associated with stripe rust (causal agent: *Puccinia striiformis* f. sp. *tritici*) resistance in wild emmer (*Triticum dicoccoides*) at the seedling stage, in the greenhouse, and at the adult plant stage, in the field. We found that the two major loci contributing to resistance in our wild emmer panel were the previously cloned seedling-stage resistance gene, *Yr15*, and the adult-plant-stage resistance gene, *Yr36*. Nevertheless, we detected 12 additional minor QTLs that additionally contribute to adult plant resistance and mapped a locus on chromosome 3AS that tentatively harbors a novel seedling resistance gene. The genotype and phenotype data generated for the wild emmer panel, together with the detected SNPs associated with resistance to stripe rust, provide a valuable resource for disease-resistance breeding in durum and bread wheat.

Keywords: GWAS; crop wild relatives; stripe rust; wheat; wild emmer; *Triticum dicoccoides*

1. Introduction

Stripe (yellow) rust is a devastating disease in wheat that is caused by the biotrophic fungus *Puccinia striiformis* f. sp. *tritici* (*Pst*). It is ranked fourth among the biotic stress factors in terms of its negative impact on yield, accounting for 2% of the annual global wheat yield losses [1]. In sub-Saharan Africa, the estimated impact of stripe rust on yield is 5%, while in western Europe, the disease results in a 6% yield loss [1], with the loss in an individual field being as high as 50% [2]. *Pst* is a highly diverse pathogen with new virulent races (pathotypes) appearing every year [3]. Because *Pst* spores are airborne and travel long distances, the pathogen can rapidly cause large-scale epidemics [2]. Currently, there are 83 designated genes and 67 provisionally designated genes for stripe rust resistance. Moreover, 61 quantitative trait loci (QTLs) have also been described for

stripe rust resistance in wheat or its wild relatives [4–6]. However, many of the known resistance genes are no longer effective, at least in some parts of the world, due to the emergence of *Pst* races that are virulent on the resistance genes used for developing widely grown commercial cultivars [3]. There are two main types of resistance to stripe rust: (i) all-stage resistance (ASR), which is usually controlled by one major R gene conferring a strong resistance response that is usually race-specific, and (ii) adult plant resistance (APR), which is effective only at the adult plant stage, is under polygenic control and is less race-specific [5]. Eighteen designated *Yr* genes confer APR, of which three have been cloned (*Yr18*, *Yr36*, and *Yr46*) [7–9]. Each of the cloned genes belongs to a different protein family. Although APR provides only partial resistance against rusts, it is considered more durable than resistance conferred by ASR, but it is more complicated to use than ASR in breeding programs, due to its polygenic nature.

Wild emmer wheat (*Triticum dicoccoides*; WEW) is the progenitor of hexaploid bread wheat (*T. aestivum*) and tetraploid durum wheat (*T. durum*), which are the most widely grown wheat crops in the world. WEW is indigenous to the Fertile Crescent, where its population is divided into a northern population (Turkey, northern Syria, Iraq, and Iran) and a southern population (Israel, the Palestinian Territories, Jordan, Lebanon, and southern Syria). Previous studies have shown that WEW was domesticated from the northern population, but there are some genetic components from the southern population [10–13]. The southern population is more diverse and is probably the origin of speciation of WEW [13–15]. At the beginning of the 20th century, WEW was proposed as a valuable genetic source for breeding by Aaronsohn (1910) [16], but the progress of transferring traits into domesticated wheat was accelerated only recently with the genome sequencing of WEW, *T. durum*, and *T. aestivum* [17–19]. Nevertheless, several stripe rust resistance genes were transferred from WEW into domesticated wheat, including *Yr36*, *Yr15*, *Yr35*, *Yr-SM139*, and additional ASR and APR genes that are described in Elkot et al. (2020) [9,20–23].

The genes *Yr15* and *Yr36* have been cloned. *Yr15* encodes a tandem kinase–pseudokinase protein (WTK1) that is located on the short arm of chromosome 1B and confers broad-spectrum ASR. Only a few very rare *Pst* races are virulent on *Yr15* [20]. *Yr15* is present in 16% of the WEW accessions from Israel, mainly from the northern part of the country, and is absent in the Fertile Crescent's northern WEW population [24]. The protein structure of the APR gene encoded by *Yr36* includes a kinase and a START lipid-binding domain (WKS1). WKS1 was shown to reduce the ability of the thylakoid-associated ascorbate peroxidase to detoxify reactive oxygen species [25]. *Yr36* is located on the short arm of chromosome 6B and is present in 67% of WEW accessions from Israel but is absent from the Fertile Crescent northern WEW population [26].

Genome-wide association studies (GWAS) have been extensively applied to cultivated crops but are far less common in crop wild relatives (CWRs). GWAS in CWRs are very challenging, due to the low levels of LD, complex population structure, and high overall background diversity [27]. To the best of our knowledge, only one GWAS study was conducted in WEW and employed the 9k SNP platform [28]. This study detected ASR-associated loci for stripe rust resistance. In cultivated wheat, many GWAS have been completed, yielding more than 80 QTLs that can be used in marker-assisted selection [5,29–33]. Most of the GWAS for adult plant stripe rust resistance in wheat used single-locus association algorithms that may not capture the multi-locus complexity of agronomic traits. However, in recent years, more GWAS to identify stripe rust APR have been using multi-locus analysis models such as FramCPU, BLINK, MMLM, and mrMLM [33–39].

In the current study, we aimed to elucidate the genetic basis of APR and ASR against stripe rust in WEW from Israel by using a GWAS, which was shown to be a powerful approach for mapping resistance genes in wheat and its wild relatives [40]. The advantage of using WEW for GWAS is the fast rate of linkage disequilibrium (LD) decay in the populations of wheat wild relatives, which increases the resolution of trait mapping [28]. We used complexity-reduced whole-genome sequencing to characterize the genetic diversity

in the WEW panel. The goals of this study were to explore the utility of WEW from Israel as the source of novel QTLs associated with ASR and APR to *Pst*.

2. Materials and Methods

2.1. Plant Material

A diversity panel of 480 WEW accessions was selected from over 2500 accessions housed at the Harold and Adele Lieberman Germplasm Bank, in the Institute for Cereal Crops Research (ICCR) at Tel Aviv University. These accessions were collected from 123 sites across Israel. Selection of the accessions was performed to maximize the geographic distribution of the species and to minimize the number of accessions originating from the same collection site. No more than eight accessions were from the same collection site. Plant passport data and the geographic distribution of accessions in the collection are presented in Table S1 and Figure S1, respectively. For the GWAS of APR, we used a subset of 188 accessions that were susceptible to race PST5006 in the seedling resistance tests (see below).

2.2. Field Trials

Field trials to assess APR to *Pst* were conducted in Israel at two locations, Zafriyya in central Israel and Barkai in northern Israel, during the cropping seasons of 2016, 2017, and 2018. In the USA, field trials were conducted at the University of California's Davis Experimental Field Station, during the cropping seasons of 2016 and 2017. In each of the trials, we planted 1–2 replicates (Table 1). Each replicate consisted of all accessions, in a completely randomized design. In total, the trial was replicated 11 times in eight field–year combinations. Seeds of the test accessions were planted in 0.3 m rows with 0.5 m spacing between the rows. Susceptible spreaders, cv. Falchetto in Israel and cv. D6301 in the Davis Experimental Field Station, were planted every 10 rows and around the field to promote stripe rust epidemics. The fields in Israel were artificially inoculated with PST5006 spores mixed with talc. Inoculation was performed every week from mid-January to mid-February. Although natural stripe rust infections occur regularly in California, we inoculated the susceptible spreader with a mixture of *Pst* spores collected at the Davis field station during the previous season to ensure strong disease pressure. We used the 0–9 infection-type (IT) scale to assess plant reactions to *Pst*, where 0 indicates a highly resistant phenotype (without visible symptoms or signs) and 9 indicates a highly susceptible phenotype, as described by Line and Qayoum (1992) [41]. Photographed scales were used as a reference [42]. Infection types (IT) on the test accessions were scored when the spreader plants were at a disease severity of 70%. Rust scoring was performed twice, approximately 2 weeks apart. Feekes growth-stage estimations were taken at the same time as the stripe rust readings [43].

Table 1. Field experiments: location, year, and the number of replicates.

Field Location	Field Name	2016	2017	2018	Geographical Location DD.DD
Barkai, ISR	BR	2 rep	2 rep	1 rep	32.47° N, 35.02° E
Zafriyya, ISR	ZA	1 rep	2 rep	1 rep	32.00° N, 34.84° E
Davis, CA, USA	US	1 rep	1 rep		38.53° N, 121.77° W

2.3. Seedling Resistance Tests

The WEW panel was screened for seedling resistance to four *Pst* isolates, as described in Huang et al. (2018) [44]. The PST5006 *Pst* isolate, representing race 38E134 (race PST5006 hereafter), originated from Israel, while the three other isolates, representing races PSTv-14, PSTv-37, and PSTv-40, originated from the United States [45,46]. Rust assays with the Israeli isolate were conducted at Tel Aviv University, whereas assays for isolates from the United States were conducted at the University of Minnesota. The rust inoculum suspension consisting of 700 µL Soltrol® oil (Chevron Phillips Chemical) and 10 mg of spores, was

sprayed onto 12-day-old plants at the two-leaf stage. Post inoculation, plants were placed inside a dew chamber at 10 °C and 100% RH for 24 h. Thereafter, for the incubation period, plants were moved into a growth chamber with a diurnal temperature cycle, gradually changing from 10 °C at 2 a.m. to 15 °C at 2 p.m., with a 16-hour photoperiod provided by high-pressure sodium lamps. Each accession was tested in three replicates. The readings were taken using the 0–9 scale, as described above. The highest IT for each accession to each race was recorded. A unified IT value for all races was calculated as the maximum IT among all races for each accession (UIT hereafter).

2.4. Genotyping

DNA was extracted from the leaves of 1-month-old plants using the DNeasy Plant Pro Kit (Qiagen), according to the manufacturer's protocol. The panel was genotyped with the genotyping by sequencing method (GBS), using *Pst*I–*Mse*I restriction enzymes [47,48]. The wild emmer Zavitan genome, version 1 (WEW_v1.0), was used as a reference [17]. Variants were called using the TASSEL GBS pipeline [49]. The genotype data were imputed using BEAGLE with all available variants [50]. For GWAS, we used only those variants and accessions that originally had less than 50% of missing data. The data were filtered for a minor allele frequency (MAF) of 1%. Variants that had more than 10% heterozygosity were removed. Filtering was performed using TASSEL v5 [49].

2.5. Yr36 and Yr15 Presence Markers

The primers WKS1_557F and WKS1_559R were used to detect the presence of *Yr36* [9]. PCR conditions were as described by Huang et al. (2016) [26]. The KASP marker Kin1 was used to detect the presence of the functional ASR gene, *Yr15* [24].

2.6. Statistical Analysis

The manipulation of data was performed using the data.table R package [51]. To test the differences between environments, we plotted a biplot using the GGEBiplotGUI R package [52]. On the basis of the observation that the differences between replicates were similar to the differences between fields (Figure 1), we considered each replicate as an environment. The best linear unbiased predictors for IT (BLUP-IT) were calculated for each accession, using the rrBLUP R package [53]. The BLUP calculation accounted for the fields (environments) and the growth stage (Feekes) as fixed effects. Broad-sense heritability (H^2) was calculated using the repeatability function within the heritability R package [54].

2.7. PCA

Principal component analysis (PCA), used to detect population structure, was based on 10% of the total variants in the genotype matrix and was performed using the pcaMethods R package [55]. Additionally, we conducted spatial PCA (sPCA), as implemented in the adegenet R package [56]. The sPCA yields scores that summarize both the genetic variability and the spatial structure among individuals [57].

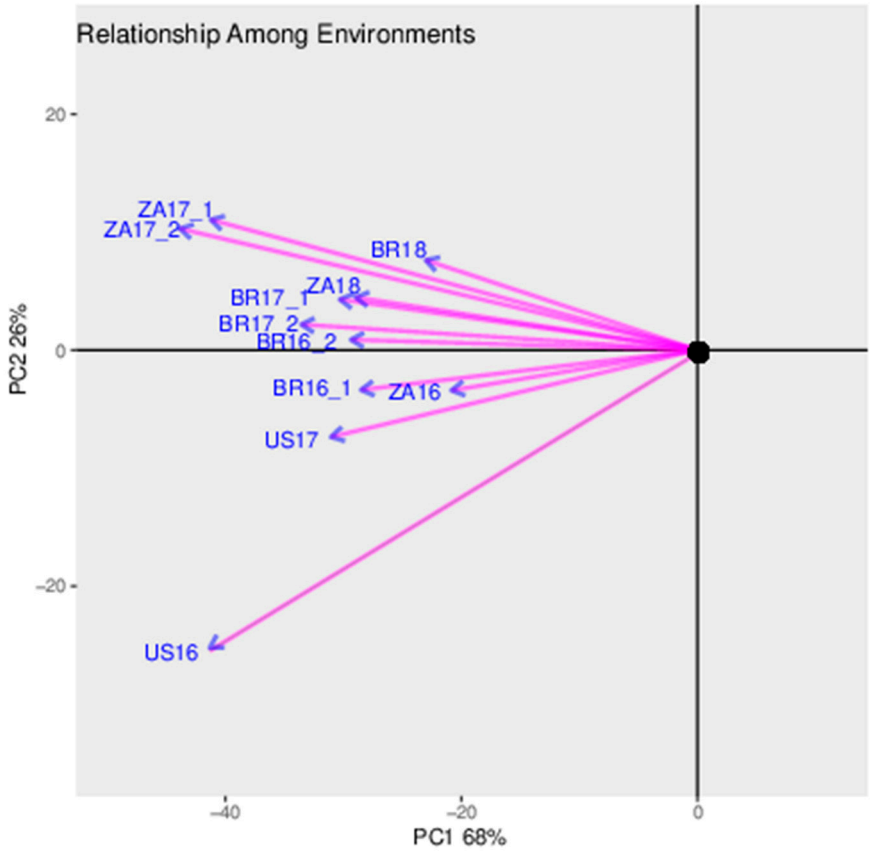

Figure 1. Environment biplot of the 11 environments (fields) used in the study, showing the relationship of IT distribution among environments. This is a genotype plus genotype-by-environment (GGE) biplot. The plot is based on the infection-type (IT) scores in the environments.

2.8. GWAS of Stripe Rust APR

The GAPIT [34] and mrMLM [35] R packages were used to detect associations between variants and BLUP-IT. We used all models of the two packages, except for GLM in GAPIT, which showed inflation of low *p*-values, and the pLARmEB method from the mrMLM package, which had a technical problem. GAPIT uses single and multi-variant detection, while mrMLM is multivariate-oriented. To correct for population structure bias, the first three principal components of PCA were used as fixed-effect covariates, and a kinship matrix was used as a random effect. The PCA and the kinship matrix were calculated using the GWAS software. On the basis of the quantile–quantile (QQ) plots, a $-\log_{10}$ *p*-value = 4 was selected as the threshold for significance (Figure 2). Above this point, *p*-values deviated from the trend line of the expected uniform distribution. The 20 best variants that had a $-\log_{10}$ *p*-value > 4 in at least two models were tested together in one mixed model, using the lmekin function from the coxme R package [58]. The model included the 20 variants as fixed effects, while the environment, accession ID, and kinship matrix of the accessions were included as random effects. The model was permuted 1000 times. Only 13 variants were significant in the mixed model, including the *Yr36* marker ($p < 0.05$). To find the best combination of subsets of the 13 variants, all possible subset combinations were tested using the lmekin fitted model within the MuMIn R function [59]. The AIC (Akaike information criterion) [60] was used as the criterion for the best combination. Interactions between variants were tested using lmekin.

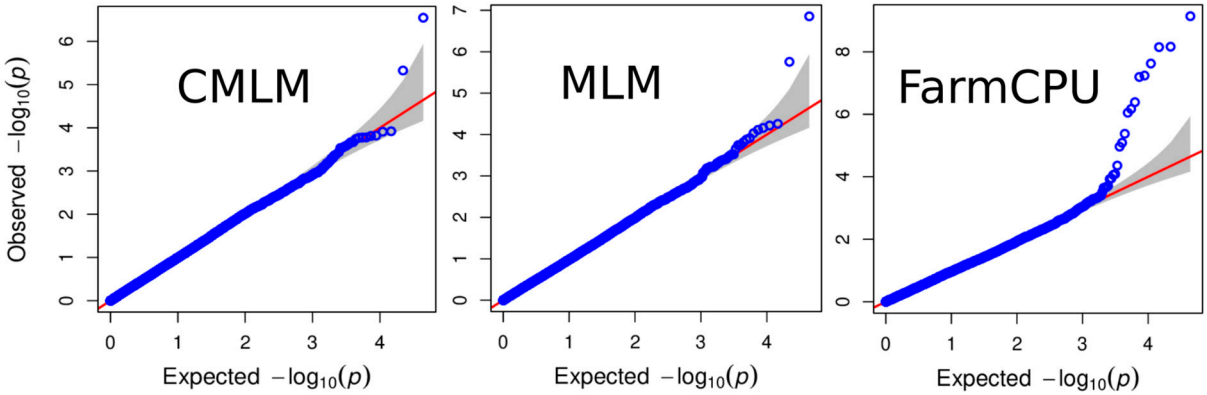

Figure 2. Quantile–quantile (QQ) plots of observed vs. expected *p*-values, obtained from the GWAS models used to detect MTA for adult plant BLUP-IT.

2.9. GWAS for ASR

GWAS was implemented for detecting the associations with ITs obtained from the seedling trials. We used all the models in GAPIT except GLM and SUPER, which demonstrated inflation in low *p*-values. We tested the reactions to each *Pst* race separately with each of the six models. The results from all runs of the individual races were collated using the data.table package in R. The association score threshold was set to a false discovery rate (FDR)-adjusted *p*-value (p_{adj}) of < 0.05 [61]. Additionally, we tested the association with UIT scores. In the latter test, we also included the SUPER model. We validated the results of the UIT association test using the ITs from each race separately. To perform this, we used a mixed model, as implemented in the lmekin function in the coxme R package, where the dependent variable was the IT for each accession (*Pst*–race combination); the variants from the two UIT significant loci (*Qpst.icci-1BS* and *Qpst.icci-3AS*) were fixed effects, and the accession ID, *Pst* race, and the kinship matrix were random effects. The model was permuted 10,000 times.

3. Results

3.1. Field Tests

The distribution of IT values across the 11 environments is presented in Figure 3 and Tables S2 and S3. The majority of the accessions had high ITs (>7), especially at the Israeli sites. ITs on accessions tested at Davis showed a more even distribution. The broad-sense heritability (H^2) for ITs was very high at 0.91. The Pearson correlation coefficients between the environments ranged between 0.39 and 0.84 (mean 0.62 ± 0.15), where the highest correlations (>0.8) were between replicates within the same field (Figure 4). The range of the BLUP values for ITs was 2.7–8.8, while BLUP values for accessions that were susceptible in the seedling test ranged between 4.0 and 8.8 (Figure 3). Twenty accessions, scored as susceptible (IT > 6) at the seedling stage, had a resistant response to stripe rust in the field experiments (BLUP-IT values < 5), suggesting that these accessions may carry levels of APR that would be useful in breeding.

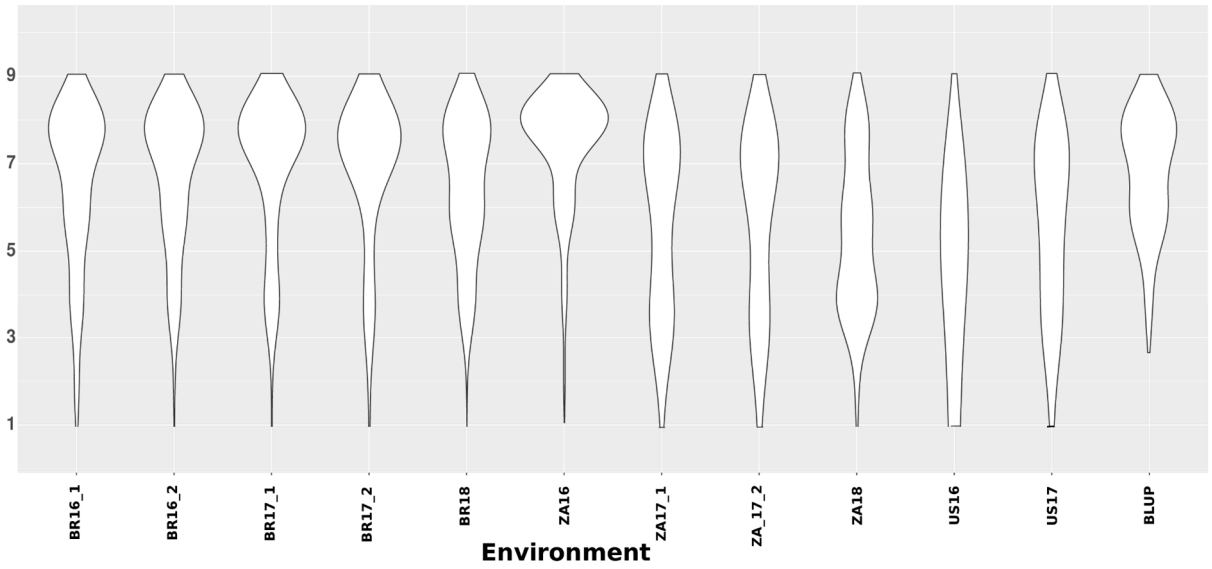

Figure 3. Violin plots showing the distribution of infection types (ITs) for stripe rust in the field trials.

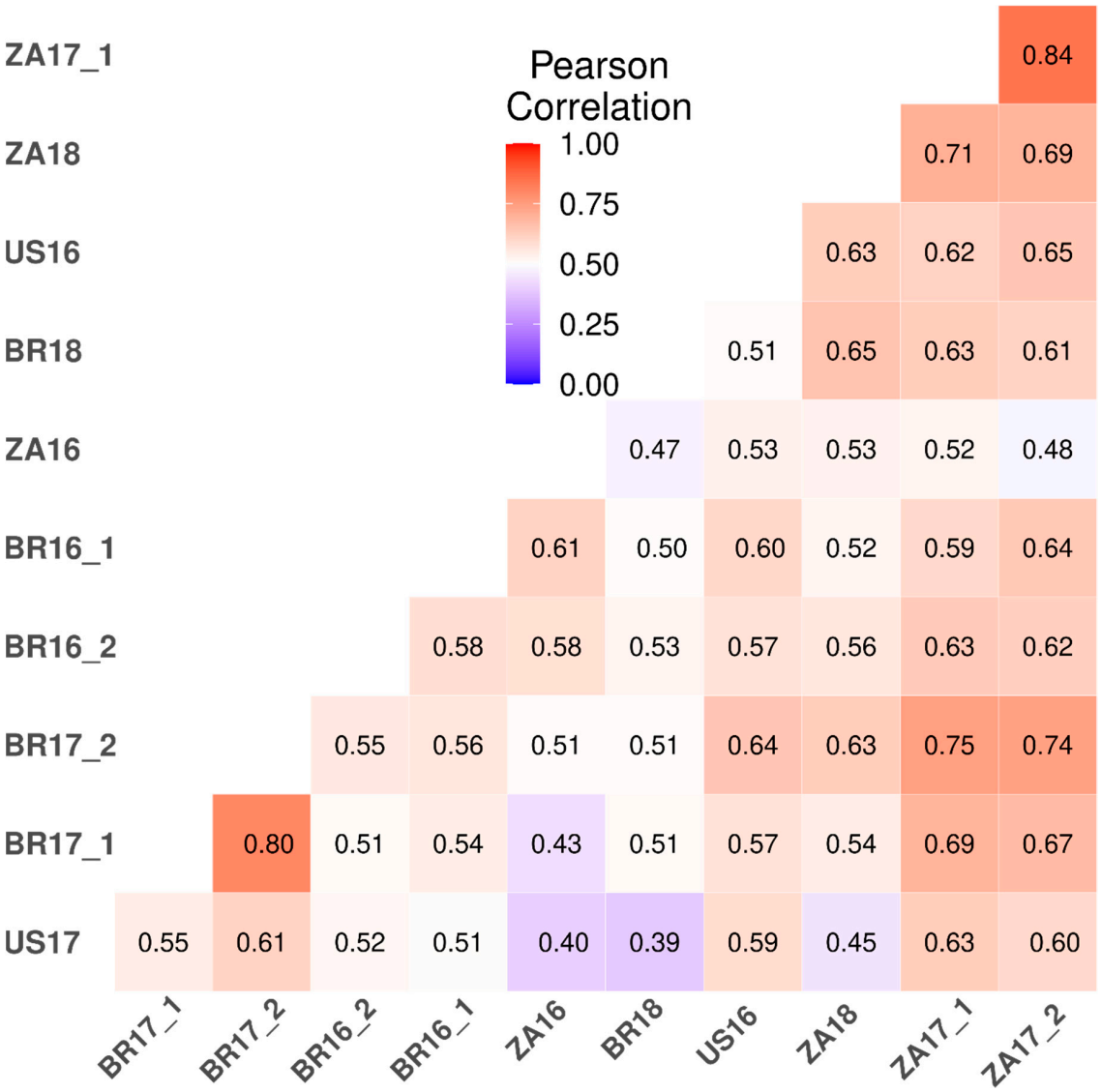

Figure 4. Correlation of IT with PST between field trials (environments).

The genotype plus genotype-by-environment (GGE) biplot showed that the differences between replicates from the same field were similar to the differences between fields (Figure 1). Therefore, we treated field replicates as different environments.

3.2. Seedling Resistance Scoring

Susceptible reactions (IT > 6) were the most common phenotypes observed. For the races PSTv-14, PSTv-37, PSTv-40, and PST5006, resistant reactions were observed in 19%, 8%, 12%, and 17% of the panel, respectively (Figure 5). The IT distribution was different among the *Pst* races. To PST5006, most of the accessions were highly susceptible (IT = 9), with only a few accessions exhibiting highly resistant reactions (IT = 1). In the case of PSTv-37, most of the accessions showed intermediate reactions, with ITs ranging between 5 and 7 (Figure 5).

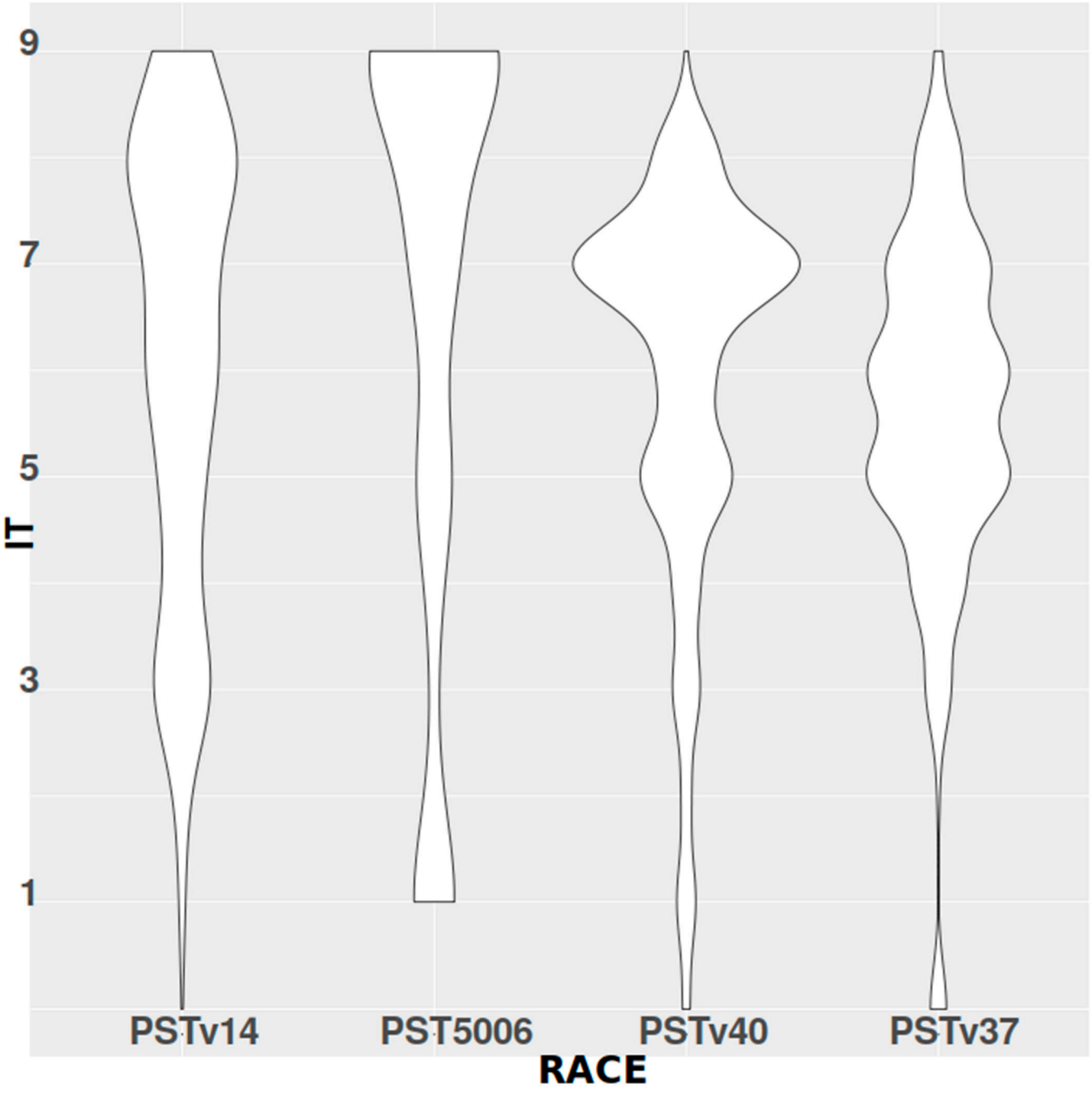

Figure 5. Violin plots showing the distribution of infection types (ITs) to stripe rust in the field trials.

3.3. Genotyping

Complexity-reduced genotyping resulted in the discovery of 341,228 variants. The entire dataset was imputed using BEAGLE with default arguments, then filtered to retain variants with MAF > 1% and a proportion of missing data in individual accessions, or SNP sites < 50% in the raw data. Using the genotypic data, we conducted PCA and identified a separate group of ~70 accessions belonging to the subgroup of *T. dicoccoides* ssp. *judaicum*. These accessions were removed from the analysis since our previous study showed that they have a substantial effect on LD that may increase the false-positive rate [28]. The final panel for the seedling resistance GWAS was composed of 419 accessions and 202,113 variants, whereas for the APR GWAS, the panel was composed of 188 accessions and 44,052 variants. Only those accessions susceptible to PST5006 were included in the APR GWAS, to avoid the masking of APR by major-effect seedling resistance genes.

3.4. Population Structure

sPCA was conducted only for the *T. dicoccoides* ssp. *horanum* accessions (those that were not detected as the *judaicum* spp.). The sPCA resulted in one PC that describes most of the spatial genetic variance. The sPCA revealed a clear geographic structure along a north–south axis, where accessions in the south were associated with positive values of PC1, while accessions from the north were associated with negative values. The accessions from the north were much more diverse than the accessions from the south (Figure S1). Superimposing APR BLUP-IT values on a PCA plot revealed that most of the resistant accessions were clustered in one corner of the plot, with negative PC1 values. This cluster originated mainly from northern Israel (Figure S2).

Linkage disequilibrium analysis revealed a rapid decay in LD along the chromosomes. Average LD values were halved from $r^2 = 0.85$ to $r^2 = 0.425$ within 800 bp and dropped below $r^2 = 0.2$ within 6 kbp and below $r^2 = 0.1$ within 150 kbp (Figure S3).

3.5. GWAS for ASR

GWAS for seedling resistance was performed using six models in the GAPIT R package for the ITs to four individual races of *Pst* (PSTv-14, PSTv-37, PSTv-40, and PST5006) and for UIT. The significance threshold was set to a FDR-adjusted *p*-value (p_{adj}) = 0.05. Two loci were associated with the UIT for all methods. One 30 Mb QTL (*Qpst.icci-1BS* hereafter) spanning several variants was identified in the distal region of the chromosome arm 1BS (63–93 Mb). The region encompassed by this QTL contains the *Yr15* locus, located close to the QTL distal border at ~65 Mb (1B:64865841) [20]. The variant with the strongest GWAS signal in *Qpst.icci-1BS* was located at ~92 Mb (1B:91719364), which is close to the proximal border of the QTL region (FarmCPU model MAF = 12%; $p_{adj} = 2.69 \times 10^{-9}$). Variants in the region within *Qpst.icci-1BS* (63–93 Mb) were associated with the presence of the functional *Yr15* gene, as determined by the *Yr15* Kin1 KASP marker, especially variant 1B:65387461 (Fisher test $p = 5.5 \times 10^{-5}$, $N = 50$). A second locus associated with IT was found on the chromosome arm 3AS at ~25 Mb (3A:25212609) (FarmCPU model, MAF = 4.5%; $p_{adj} = 5.38 \times 10^{-10}$; Figure S4; *Qpst.icci-3AS* hereafter). The seedling IT effect of the two marker-trait associations (MTAs) differed significantly from race to race. The highest effects were observed for race PST5006 (5.4–5.2), while for race PSTv-37, the effects were much lower (1.6–1.8; Figure S5). The distributions of effects for each of the two QTLs were similar (1.5–5.5). We tested the two QTLs together in a mixed model using the lmekin R function, where the dependent variable was the IT for each accession. Variants from *Qpst.icci-1BS* and *Qpst.icci-3AS* were set as fixed effects. The accession ID, *Pst* race, and kinship matrix were set as random effects. The model was permuted 10,000 times. *Qpst.icci-1BS* and *Qpst.icci-3AS* were significantly associated with IT in the original model ($p = 0$ and $p = 17 \times 10^{-5}$, respectively) and after the permutation test analysis ($p < 0.0001$ and $p = 0.002$, respectively). Three accessions with no favorable alleles in *Qpst.icci-1BS* and *Qpst.icci-3AS* were resistant (IT < 5) to all the *Pst* races tested. Because they do not carry the *Yr15* favorable allele and still show a broad resistance to *Pst*, these accessions from Central

Samaria, Lower Galilee, and Golan Heights can be used for discovering new *Pst* resistance loci other than *Yr15*.

From the GWAS results conducted for each race separately, we removed the results of PSTv-40 tested with the single-variant models, namely, MLM, CMLM, and ECMLM, as well as all results from the SUPER model since the QQ plots showed inflated low *p*-values for these analyses (Figure S6). The remaining results did not converge to a single significant variant across all races and all models. However, all race × model combinations showed association signals in the *Qpst.icci-1BS* region (63–93 Mb). This genomic region, harboring the *Yr15* locus, has high LD levels (Figure S7). The highest association values were obtained by the multi-locus models Blink, FarmCPU, and MMLM for variant 1B:66240332, which was associated with the IT of PSTv-40 (p_{adj} = 3.2 × 10^{-82}, 3.9 × 10^{-33}, and 2.5 × 10^{-16}, respectively). The same variant was also highly associated with ITs to PST5006, according to FarmCPU (p_{adj} = 1.9 × 10^{-9}). FarmCPU revealed a strong association of ITs to PSTv-37 with a nearby locus (1B:72049807, p_{adj} = 8.0 × 10^{-14}, Table 2).

Table 2. Association estimates of IT in the seedling stage for each *Pst* race. Variants were clustered into 40 Mb windows using Zavitan WEW_v1.0 as a reference genome. [1] Markers were aligned to QTL data from Wang and Chen (2017) [5].

Chr	40 Mb Window Center Mb	No. of Race/Model Combinations Significant Results	*Pst* Race List	Models	Max −log10(*p*)	Max −log10(p_{adj})	Aligned QTL [1] [5]
1B	80	12	37, 40, 5006, 14	Blink, CMLM, FarmCPU, MLMM	86.83	81.52	*Yr15* [20]
1A	560	3	5006, 37	Blink, CMLM, FarmCPU	30.83	25.52	Q.1A.9 [62]
4B	640	4	5006	Blink, CMLM, FarmCPU	21.73	16.72	Q.4B.14 [63]
3A	680	3	5006	Blink, CMLM, FarmCPU	15.25	9.94	
2A	120	6	37	Blink, CMLM, ECMLM, FarmCPU, MLMM, MLM	9.25	4.15	Q.2A.17 [64]
3A	720	5	5006, 37	Blink, CMLM, ECMLM, MLMM, MLM	8.44	3.43	
4A	160	3	14	ECMLM, MLMM, MLM	7.72	2.42	
2B	160	4	37	CMLM, ECMLM, FarmCPU, MLM	6.68	2.26	*Yr31* [65]
1A	320	4	37	Blink, CMLM, ECMLM, MLM	6.54	1.84	
5B	120	9	37	CMLM, ECMLM, MLM	6.08	1.62	
1B	560	3	37, 5006	Blink, FarmCPU	5.79	1.47	*Yrv3* [66]

3.6. GWAS for APR

The GWAS for APR-associated loci was performed using 11 methods from the GAPIT and mrMLM packages [34,35]. The GLM method from the GAPIT package was not included

because of an inflated low *p*-value distribution. The pLARmEB method from the mrMLM package was not used due to technical problems.

Twenty significant variants were detected by at least two methods ($-\log_{10}$ *p*-value > 4). The only marker that was detected using all methods was the PCR marker for *Yr36* (Table 3). No significant variants from the GBS matrix were found near the *Yr36* locus, probably because the gene region is deleted in the Zavitan reference genome [9,17]. To further test the significance of the markers, we included all of them as fixed variables in a mixed model using the IT scores from each of the 11 environments. The kinship matrix, environment (field), and genotype ID were used as random variables. The mixed model detected 13 significant markers, including the *Yr36* marker ($p < 0.005$). All 13 markers remained highly significant ($p < 0.001$) after further testing of the model by 1000 permutations.

Table 3. Variants that are significantly associated with adult plant resistance. The results of GWAS with various models and results of mixed models, with all variants together, using the coxme::lmekin R function.

Variants	Minimum *p*-Value of GWAS	GWAS Models	Estimate lmekin	*p*-Value lmekin	Aligned QTL [1] [5,6]	Putative Genes [2]
1A_571777232	9.20×10^{-9}	mrMLM, FASTmrMLM, pKWmEB	−0.198	1.30×10^{-4}	Q.1A.9 15% [3] F [4] [62]	TRIDC1AG060480 WRKY domain [67]
1B_39276972	2.15×10^{-10}	mrMLM, FASTmrMLM	0.390	1.10×10^{-12}	MQTL4-1B 15% F [6]	TRIDC1BG006690 Papain-like cysteine peptidase [68]
3B_550434503	7.03×10^{-15}	FASTmrMLM, FASTmrEMMA	−0.295	6.20×10^{-5}	Q.3B.24 6% F [69]	TRIDC3BG050030 Eukaryotic translation initiation factor 3 subunit eif-3 [70]
3B_707838360	9.82×10^{-10}	FarmCPU, MLM, BLINK, mrMLM, FASTmrMLM	−0.221	1.80×10^{-3}		TRIDC3BG067020 Peptidase A22B, signal peptide peptidase [71]
3B_88645297	5.40×10^{-5}	ECMLM, MLMM, SUPER	−0.190	2.70×10^{-3}	Q.3B.8 6% F [72] Q.B3.9 20% F [73] Q.3B.10 5% F [74] Q3B.12 30% F [75] Q3B.14 5% F [65]	TRIDC3BG015830 alpha/beta hydrolase fold [76]
5B_157144166	8.75×10^{-8}	mrMLM, FASTmrMLM, pKWmEB	0.371	2.30×10^{-7}	Q.5B.2 6% F [77]	TRIDC5BG018210 AIG1-type guanine nucleotide-binding [78]
5B_24593659	3.12×10^{-10}	mrMLM, FASTmrMLM	−0.337	1.30×10^{-8}	Q5B.2 6% F [77] Q5B.3 27% [79]	TRIDC5BG004210 Methyl-CpG DNA binding [80]
5B_527982577	2.32×10^{-12}	mrMLM, FASTmrMLM	0.205	2.30×10^{-4}	Q.5B.18 33% [81] Q5B.19 3% F [82] Q5B.20 30% F [83]	TRIDC5BG053620 NAC domain [84]
6B_132922231	1.60×10^{-7}	FASTmrEMMA, pKWmEB	−0.221	3.30×10^{-3}	Q.6B.3 15% F [62] Q.6B.6 35% F [85] Q.6B.7 6% F [86]	TRIDC6BG018950 NB-ARC [87]
6B_138700000_*Yr36*	3.25×10^{-23}	CMLM, ECMLM, FarmCPU, MLM, MLMM, SUPER, BLINK, mrMLM, FASTmrMLM, pKWmEB, ISIS EM-BLASSO	−0.792	7.70×10^{-12}	*Yr36 F* [9]	*kinase_START*

Table 3. *Cont.*

Variants	Minimum *p*-Value of GWAS	GWAS Models	Estimate lmekin	*p*-Value lmekin	Aligned QTL [1] [5,6]	Putative Genes [2]
6B_664322346	4.74×10^{-5}	ECMLM, MLMM, SUPER	−0.206	3.90×10^{-4}	Q.6B.16 Q.6B.17 Q.6B.18 [5]	TRIDC6BG064680 WD repeat HIR1 [88]
7A_501622609	5.75×10^{-13}	FASTmrMLM, pKWmEB	0.260	5.00×10^{-6}	Q.7A.9 6% F [89]	TRIDC7AG048010 Ubiquitin-Conjugating Enzyme E2 [90]
7B_105138786	6.93×10^{-11}	mrMLM, FASTmrEMMA	−0.390	5.60×10^{-9}		TRIDC7BG013060 Cellulose Synthase Interactive [91]

[1] Markers were aligned to QTL data from Wang and Chen 2017 [5] and Jan et al. (2021) [6] (Figure S9). [2] The putative genes are the closest genes to the SNP that have some relation to disease resistance or the regulation of expression. The putative function is given under the gene name from wild emmer genome annotation v1 [17]. [3] Percentage of explained variation of the cited QTL. [4] Indication that the QTL was found in a field experiment.

To ensure that the model was not overfitted, we used an Akaike information criterion (AIC) wherein all possible subset combinations of the 13 loci were tested. The full model had the lowest AIC, meaning it was the best model to describe the association of the 13 loci with ITs. We used a similar mixed model to test the variance explained by the different components. In this model, we tested the BLUP-ITs instead of the ITs of each field, to exclude field variations from the model. The pseudo-*R*-squared calculation, using the likelihood-ratio test, showed that the 13 genetic loci explained 83% of the variance, of which one-quarter was explained by *Yr36* and the rest by the other 12 loci. A similar mixed model was also used to test for interactions between *Yr36* and the other 12 variants; however, no significant interactions were detected ($p > 0.05$). The number of favorable alleles (i.e., alleles associated with IT reduction) in each genotype was calculated on the basis of the 12 variants and plotted against the BLUP-IT, once for genotypes with *Yr36* and once for genotypes without *Yr36*. The trend in both cases showed a clear negative correlation between the number of favorable alleles and the mean BLUP-IT, where genotypes with *Yr36* had lower BLUP-IT than those without *Yr36* (Figure 6). The interactions of the 12 variants and *Yr36* were visualized using boxplots (Figure S8). In 10 of the variants, the effect of the favorable allele was larger in the presence of *Yr36*. Looking at the results from a different perspective, it was evident that all of the variants enhanced the positive effect of *Yr36* on resistance. The distribution of the 13 loci along the genome was uneven, with most (11) being detected in the B-genome chromosomes (1B and 7B, each with one; 3B, 5B, and 6B, each with three) and two in chromosomes from the A genome (1A and 7A, each with one).

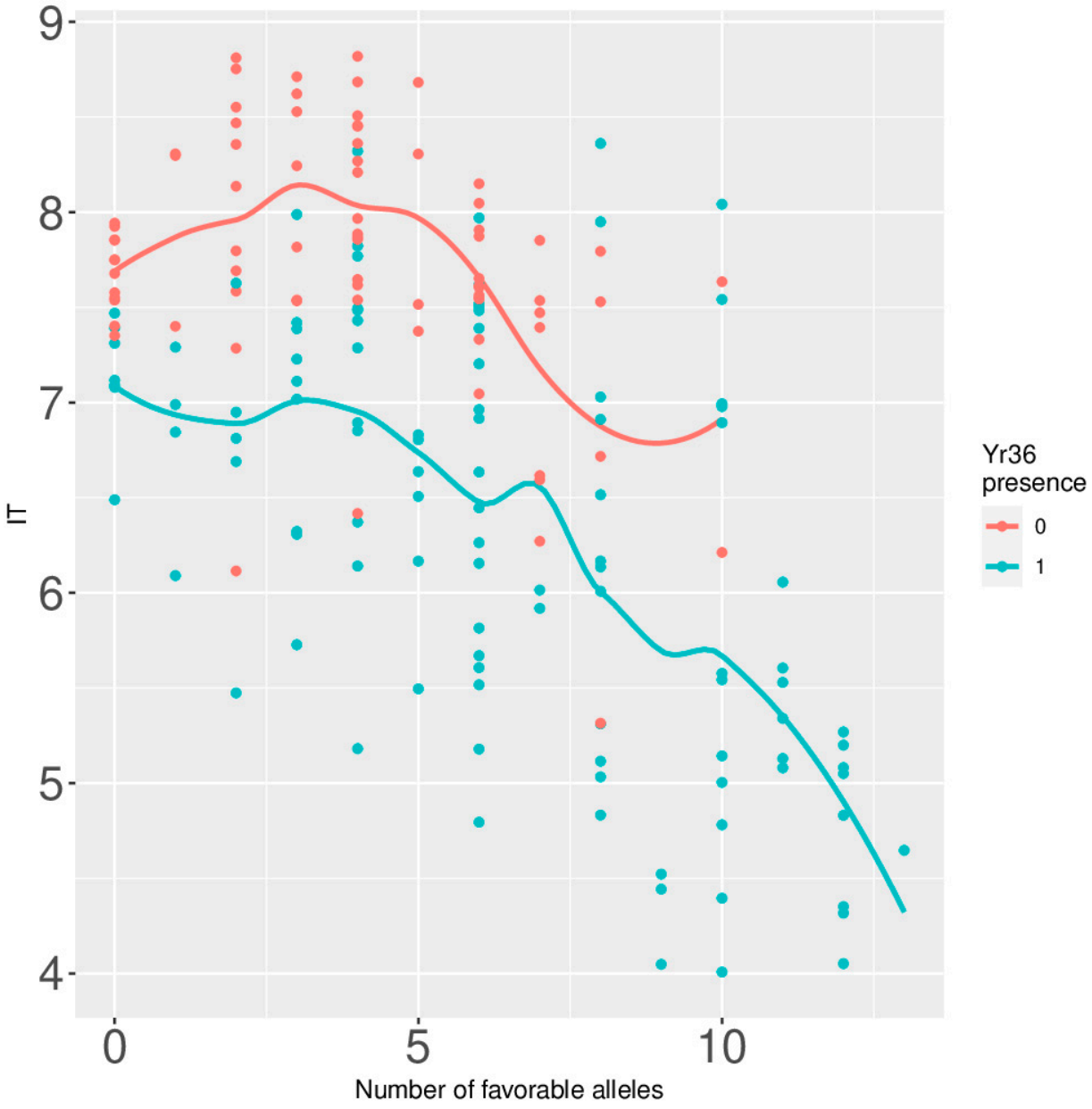

Figure 6. Correlation of infection types with the number of favorable alleles in wild emmer accessions. Colors indicate the presence (1, blue line and dots) and the absence (0, red line and dots) of *Yr36* in the genotype. *Y*-axis: BLUP values for infection types (BLUP-IT); *X*-axis: number of favorable (reducing IT) alleles of the 12 significant loci in each accession.

4. Discussion

The main goals of this study were to identify the loci associated with stripe rust resistance at the seedling stage (ASR) and the adult plant stage (APR), and to identify accessions that may carry novel APR or ASR resistance genes.

4.1. LD Levels

Linkage disequilibrium (LD) levels in the wild emmer population decayed very rapidly, within the first 1 kb, as r^2 values were halved from ~0.85 to 0.425. This rapid decay was observed in the same population, using the 9k SNP array [29], and in another WEW panel and a wild barley panel, using Sanger sequencing [92,93]. These LD estimates are much lower than the estimates in the selfing wild population of *Arabidopsis thaliana*, where LD decayed within 250 kb [94]. The estimates of LD extent in wild populations

are several times lower than the LD extent in domesticated wheat, where LD can extend several centimorgans [38,95]. These low LD levels are favorable, in the sense that they increase the resolution of GWAS; however, a much higher marker density is required in the panel to detect significant associations [95].

4.2. All-Stage Resistance

The ASR GWAS identified two loci that were associated with UIT, indicating that they confer resistance to all four *Pst* races. *Qpst.icci-1BS* (63–93 Mb) colocalizes with the *Yr15* locus [20]. This QTL extends over a wide interval, and LD analysis indicates that high LD levels in the region may be the reason (Figure S7). Therefore, it is highly probable that all of the associations found in this region are caused by *Yr15*. However, the most significant associations from the GWAS did not identify the closest variant to the *Yr15* locus. Testing for associations between *Qpst.icci-1BS* variants and the *Yr15* KASP marker detected variants closer to the *Yr15* locus than the GWAS results, based on ITs. This means that the GBS-based GWAS in wild populations are limited in their precision, probably because of missing data, low allele frequencies, and variations in the phenotypic expression of resistance, due to the large diversity in the genetic background of accessions. This result may also suggest that other ASR genes are located in *Qpst.icci-1BS* but are masked by *Yr15* and the LD block.

Qpst.icci-3AS (~25 Mb) is located in the same region as *Yr76*. This gene originated from the hexaploid club wheat cultivar, Tyee, which includes in its pedigree a stripe rust-resistant *T. durum* landrace from Ethiopia [96,97]. *Yr76* is genetically located 2.3 cM proximal to wmc11, which is physically located at ~168 Mb of chromosome 3A in the Zavitan WEW_v1.0 reference genome (3AS:16784689) [98]. We cannot rule out the possibility that *Yr76* and *Qpst.icci-3AS* are at the same locus. *Qpst.icci-3AS* overlaps with Q3A.1, a QTL that was observed only once in one environment, probably originating from cv. Sarr (Figure S9) [5,99]. *Qpst.icci-3AS* is located between two copies of genes encoding a wall-associated receptor kinases (TRIDC3AG005570 and TRIDC3AG005580), which are located 60 kb apart. These genes may be involved in resistance to stripe rust [100,101].

Of the 10 race-specific loci, five loci were aligned with previously reported QTLs or genes, including *Yr31* and *Yrv3* (Table 2, Figure S9) [5].

Additional resistance genes may also be present in the WEW population from Israel. However, the masking effect of *Yr15*, coupled with the low frequency of these putative genes, likely complicates their detection by GWAS. Nevertheless, we identified several accessions that do not have favorable alleles at these two QTLs, which may be useful for biparental linkage analysis.

The effect of the two QTLs, detected on the basis of UITs, was highly dependent on the *Pst* race used in the assay. For PST5006, the effect of the favorable allele of either locus on the IT was a shift from highly susceptible to highly resistant, while for PSTv-37, the shift was from moderately susceptible to moderately resistant. For PSTv-14 and PSTv-40, the IT shift was intermediate (Figure S5). This observation underlines the importance of using multiple pathogen races in plant resistance studies and reveals that the host-pathogen interactions are affected not only by virulence/avirulence patterns but also by varying aggressiveness in the pathogen.

4.3. Adult Plant Resistance

The GWAS for APR revealed that the main locus determining this trait in the WEW panel from Israel is *Yr36*. However, the level of resistance is also affected by at least 12 additional minor-effect loci that have an additive effect. We observed that *Yr36* alone does not explain most of the variance in resistance to *Pst* of the WEW population.

Wang and Chen (2017) reported on 327 QTLs for stripe rust resistance in wheat, with many overlaps (Figure S9). More than 80 of these QTLs were identified using GWAS [5], and many were identified in field trials, suggesting that they may confer APR. Numerous additional QTLs for APR to *Pst* have been detected since 2017 [30–33,66]. We aligned

the APR GWAS results with those QTLs reported in the QTL reviews of Wang and Chen (2017) and Jan et al. (2021) (Figure S9) [5,6]. We found that 3 of the 13 APR loci do not align with any previously identified QTL and, therefore, may be novel (Table 3). The remaining loci were aligned to previously published QTLs, with most being identified in field trials. However, many of these QTLs had large confidence intervals, were mapped against different genomes using a different panel or mapping population, or employed a different marker system. Therefore, it is difficult to determine with certainty whether the loci detected in the current study are allelic to previously published QTLs. However, we found several loci with a precise alignment to previously published narrow QTLs, potentially indicating that the loci from the current study are allelic to the previously published QTLs. These loci were 3B:88645297, which aligned with five QTLs, and with *Yr4*, which is not an APR gene [5], 5B:527982577, which aligned with three narrow APR QTLs, and the locus on 6B:664322346, which aligned with three APR QTLs [5] (Table 3, Figure S9). Nevertheless, none of the previously published QTLs originated directly from WEW. We searched for candidate genes in the vicinity of the SNPs (up to 1 Mbp) using WEWv1 annotation. We found genes that are involved in disease perception, such as NB-ARC and WD repeat HIR1; genes that are involved in regulation, such as WRKY and NAC; genes controlling cell-wall biosynthesis, such as cellulose synthase; genes controlling the ubiquitination of a pathogen effector (ubiquitin-conjugating enzyme); and genes controlling epigenetic regulation (methyl-CpG-binding domain) (Table 3).

4.4. The Effect of Diverse Genetic Background on Major Gene Resistance

The two main *Yr* genes in the WEW Israeli gene pool are *Yr15* for ASR and *Yr36* for APR. Other resistance genes may be present, but their frequencies were too low to be detected by GWAS. However, we can detect resistant accessions that do not have the *Yr15* or *Yr36* favorable alleles and cross them with a susceptible genotype to isolate the gene. The range of ITs observed in accessions that have *Yr15* or *Yr36* was wide. This indicates that the effects of these genes on *Pst* infection are impacted by the genotypic background. For *Yr36*, we showed that its effect is dependent on at least 12 other loci. We also know from our own observations that the effect of *Yr15* in its original source (accession G25) and in hexaploid wheat with *Yr15* introgressions (such as Avocet-*Yr15*) is much stronger than what we have observed in the WEW panel in the field. These observations suggest that the discovery of novel resistance genes, especially those conferring APR, may be complicated by the highly heterogeneous background of accessions in wild populations.

4.5. Performance of GWAS Methods

We used two R packages for the GWAS of APR in WEW. Each package includes several GWAS methods. The mrMLM package has models for multiple variants, while GAPIT has models for single variants, as well as for multiple variants [34,35]. In the APR GWAS, 9 out of the 13 variants were detected only by multiple-variant methods from the mrMLM package, while only 2 variants were detected by GAPIT methods alone, and 2 variants were detected by both packages. It seems that the mrMLM package, which uses multivariant models, is better at detecting variants in the WEW quantitative APR GWAS. Our approach to detect MTAs consisted of three steps: (i) detecting the trait-associated variants by applying multiple GWAS models, either for multiple variants or single variants; (ii) validating and filtering the detected variants using a mixed model that tests all selected variants in one model and accounts for genotype relatedness and the variation between environments, with validation by permutation analysis; (iii) selecting the model with the best combination of variants based on the AIC criterion. This approach may help to overcome the reduction in the power of GWAS tests caused by the heterogeneity of genetic backgrounds in wild populations. Moreover, adding the environment (field) variance into the mixed model enhances the robustness of the model, leading to more reliable results. To the best of our knowledge, this is the first time that this combination of steps has been used for GWAS validation. We believe that this combination of analytical steps will enhance the

power of GWAS and reduce false associations. For the ASR GWAS, we used only those models that were implemented in the GAPIT package since we were expecting single-gene resistance. In our study, the best-performing models were MMLM, FarmCPU, and Blink, which are multiple-variant models. The single-variant models (e.g., MLM, CMLM, and ECMLM) resulted in high *p*-values with more noise, while the SUPER and GLM models generated inflated low *p*-values (Figure S6).

5. Conclusions

We demonstrated that multiple-variant GWAS methods are able to detect major and minor resistance genes in wild wheat populations, using the GBS approach. However, we see value in increasing the marker density in genetically diverse populations of wild relatives, beyond the density provided by GBS technology, to increase the rate of marker-trait association discovery. As demonstrated, reference- and GBS-based GWAS may miss key resistance genes due to the absence of the gene in the reference genome and due to very low LD levels. The advances in sequencing technologies and the drop in sequencing costs may facilitate high-resolution reference-free GWAS that can overcome these limitations.

Supplementary Materials: The following supporting information can be downloaded at https://www.mdpi.com/article/10.3390/crops2010005/s1: Table S1. Infection type data and passport data of the association panel; Table S2. ITs of the accessions; Table S3. Summary statistics of ITs from the fields; Figure S1. Geographical distribution of wild emmer genotypes in Israel and its vicinity. Colors represent the assignment of the genotype to a bin along the first principal component, as calculated by sPCA. Pie represents the proportion of genotypes assigned to the bins within 20 × 20 km. The size of the pie is proportional to the number of genotypes; Figure S2. PCA based on the GBS matrix of the wild emmer population. Colors represent BLUP-IT to *Pst* at the adult plant stage; Figure S3. Linkage disequilibrium (LD) levels along the wild emmer genome. Left, distance 0–10 kbp; Right, distance 0–1 Mbp; each dot is the mean of a 100 bp window. Blue line, Loess averaging; Figure S4. Circular Manhattan plot of the associations with UIT at the seedling stage, using seven GWAS models. Red stars indicate significant associations after Bonferroni correction ($\alpha = 0.01/N$); Figure S5. Seedling ITs in four *Pst* races partitioned into alleles in the two significant seedling resistance MTAs. The length of the line is proportional to the number of accessions with the same IT; Figure S6. QQ plots of GWAS results using the SUPER model with the seedling IT; Figure S7. Linkage disequilibrium r^2 estimates near the *Yr15* locus on 1BS; Figure S8. Level of BLUP-IT at the adult plant stage. For each of the 12 significant loci, ITs are partitioned into four boxplots by the *Yr36* X allele combination; Figure S9. Chromosomal locations of wheat genes or quantitative trait loci (QTLs) for resistance to stripe rust. Resistance genes with permanent and provisional *Yr* symbols are shown on the left, and QTLs are shown on the right of each chromosome. QTLs are coded by numbers and can be found in Table 5.4 of Wang and Chen (2017) [5]. Loci detected in the current study are indicated by colored boxes: red—APR; green—ASR UIT (unified IT); blue—ASR race-specific loci. The figure is based on Figure 5.1 in from Wang and Chen (2017) [5].

Author Contributions: M.T. conducted the field experiments in Israel and was assisted by J.R. for data collection. E.A. (Elina Adhikari) and K.W.J. conducted the GBS analysis. N.C., I.A.d.B. and X.C. conducted the field experiments in the USA. O.M., J.M. and P.B.Y. conducted the seedling experiments. X.C. donated the North American *Pst* races. S.E. extracted the DNA. S.E. and L.G. conducted molecular marker analysis. B.S., E.A. (Eduard Akhunov) and H.S. conceptualized the study, wrote the grant proposal, and supervised the experiments. H.S. conducted the statistical analysis and wrote the paper. All authors have read and agreed to the published version of the manuscript.

Funding: This research was funded by the BARD IS-4744-14 project and in part by the Lieberman–Okinow Endowment at the University of Minnesota and the Minnesota Agricultural Experiment Station Project No. MIN-22-085: Exploiting Wild Relatives for Cultivated Wheat and Barley Improvement. E. Adhikari was also supported by the Bill and Melinda Gates Foundation (INV-004430).

Data Availability Statement: The raw reads of the GBS analysis were deposited to the SRA archive (https://www.ncbi.nlm.nih.gov/sra) under project PRJNA751112. Infection type data and passport data are available in Supplementary Table S1.

Acknowledgments: We thank Tamas Szinyei from the University of Minnesota and Oxana Maatuk and Sophie Klausner from Tel Aviv University for their excellent technical assistance. We thank Roi Ben David and Imri Kayts for the free use of the fields in Zafriyya and Barkai respectively.

Conflicts of Interest: The authors declare no conflict of interest.

References

1. Savary, S.; Willocquet, L.; Pethybridge, S.J.; Esker, P.; McRoberts, N.; Nelson, A. The global burden of pathogens and pests on major food crops. *Nat. Ecol. Evol.* **2019**, *3*, 430–439. [CrossRef] [PubMed]
2. Chen, X. Pathogens which threaten food security: *Puccinia striiformis*, the wheat stripe rust pathogen. *Food Secur.* **2020**, *12*, 239–251. [CrossRef]
3. Liu, T.; Wan, A.; Liu, D.; Chen, X. Changes of Races and Virulence Genes in *Puccinia striiformis* f. sp. *tritici*, the Wheat Stripe Rust Pathogen, in the United States from 1968 to 2009. *Plant Dis.* **2017**, *101*, 1522–1532. [CrossRef] [PubMed]
4. Catalogue of Wheat Gene Symbols. Available online: https://shigen.nig.ac.jp/wheat/komugi/genes/symbolListPageAction.do?page=-1 (accessed on 18 November 2021).
5. Wang, M.; Chen, X. Stripe Rust Resistance. In *Stripe Rust*; Springer: Berlin/Heidelberg, Germany, 2017; pp. 353–558.
6. Jan, I.; Saripalli, G.; Kumar, K.; Kumar, A.; Singh, R.; Batra, R.; Sharma, P.K.; Balyan, H.S.; Gupta, P.K. Meta-QTLs and candidate genes for stripe rust resistance in wheat. *Sci. Rep.* **2021**, *11*, 22923. [CrossRef] [PubMed]
7. Krattinger, S.G.; Lagudah, E.S.; Spielmeyer, W.; Singh, R.P.; Huerta-Espino, J.; McFadden, H.; Bossolini, E.; Selter, L.L.; Keller, B. A Putative ABC Transporter Confers Durable Resistance to Multiple Fungal Pathogens in Wheat. *Science* **2009**, *323*, 1360–1363. [CrossRef]
8. Milne, R.J.; Dibley, K.E.; Schnippenkoetter, W.; Mascher, M.; Lui, A.C.; Wang, L.; Lo, C.; Ashton, A.R.; Ryan, P.R.; Lagudah, E.S. The Wheat *Lr67* Gene from the Sugar Transport Protein 13 Family Confers Multipathogen Resistance in Barley. *Plant Physiol.* **2018**, *179*, 1285–1297. [CrossRef]
9. Fu, D.; Uauy, C.; Distelfeld, A.; Blechl, A.; Epstein, L.; Chen, X.; Sela, H.; Fahima, T.; Dubcovsky, J. A Kinase-START Gene Confers Temperature-Dependent Resistance to Wheat Stripe Rust. *Science* **2009**, *323*, 1357–1360. [CrossRef]
10. He, F.; Pasam, R.; Shi, F.; Kant, S.; Keeble-Gagnere, G.; Kay, P.; Forrest, K.; Fritz, A.; Hucl, P.; Wiebe, K.; et al. Exome Sequencing Highlights the Role of Wild-Relative Introgression in Shaping the Adaptive Landscape of the Wheat Genome. *Nat. Genet.* **2019**, *51*, 896–904. [CrossRef]
11. Luo, M.-C.; Yang, Z.-L.; You, F.M.; Kawahara, T.; Waines, J.G.; Dvorak, J. The structure of wild and domesticated emmer wheat populations, gene flow between them, and the site of emmer domestication. *Theor. Appl. Genet.* **2007**, *114*, 947–959. [CrossRef]
12. Nave, M.; Avni, R.; Çakır, E.; Portnoy, V.; Sela, H.; Pourkheirandish, M.; Ozkan, H.; Hale, I.; Komatsuda, T.; Dvorak, J.; et al. Wheat domestication in light of haplotype analyses of the Brittle rachis 1 genes (*BTR1-A* and *BTR1-B*). *Plant Sci.* **2019**, *285*, 193–199. [CrossRef]
13. Özkan, H.; Willcox, G.; Graner, A.; Salamini, F.; Kilian, B. Geographic distribution and domestication of wild emmer wheat (*Triticum dicoccoides*). *Genet. Resour. Crop Evol.* **2010**, *58*, 11–53. [CrossRef]
14. Feldman, M.; Kislev, M.E. Domestication of emmer wheat and evolution of free-threshing tetraploid wheat. *Isr. J. Plant Sci.* **2007**, *55*, 207–221. [CrossRef]
15. Nevo, E.; Korol, A.B.; Beiles, A.; Fahima, T. *Evolution of Wild Emmer and Wheat Improvement: Population Genetics, Genetic Resources, and Genome Organization of Wheat's Progenitor, Triticum dicoccoides*; Springer Science & Business Media: Berlin/Heidelberg, Germany, 2002; ISBN 978-3-540-41750-7.
16. Aaronsohn, A. *Agricultural and Botanical Explorations in Palestine*; US Government Printing Office: Washington, DC, USA, 1910.
17. Avni, R.; Nave, M.; Barad, O.; Baruch, K.; Twardziok, S.O.; Gundlach, H.; Hale, I.; Mascher, M.; Spannagl, M.; Wiebe, K.; et al. Wild emmer genome architecture and diversity elucidate wheat evolution and domestication. *Science* **2017**, *357*, 93–97. [CrossRef] [PubMed]
18. The International Wheat Genome Sequencing Consortium (IWGSC); Appels, R.; Eversole, K.; Stein, N.; Feuillet, C.; Keller, B.; Rogers, J.; Pozniak, C.J.; Choulet, F.; Distelfeld, A.; et al. Shifting the limits in wheat research and breeding using a fully annotated reference genome. *Science* **2018**, *361*, 7191. [CrossRef]
19. Maccaferri, M.; Harris, N.S.; Twardziok, S.O.; Pasam, R.K.; Gundlach, H.; Spannagl, M.; Ormanbekova, D.; Lux, T.; Prade, V.M.; Milner, S.G.; et al. Durum wheat genome highlights past domestication signatures and future improvement targets. *Nat. Genet.* **2019**, *51*, 885–895. [CrossRef]
20. Klymiuk, V.; Yaniv, E.; Huang, L.; Raats, D.; Fatiukha, A.; Chen, S.; Feng, L.; Frenkel, Z.; Krugman, T.; Lidzbarsky, G.; et al. Cloning of the wheat *Yr15* resistance gene sheds light on the plant tandem kinase-pseudokinase family. *Nat. Commun.* **2018**, *9*, 3735. [CrossRef]
21. Marais, G.F.; Pretorius, Z.A.; Wellings, C.R.; McCallum, B.; Marais, A.S. Leaf rust and stripe rust resistance genes transferred to common wheat from *Triticum dicoccoides*. *Euphytica* **2005**, *143*, 115–123. [CrossRef]
22. Zhang, H.; Zhang, L.; Wang, C.; Wang, Y.; Zhou, X.; Lv, S.; Liu, X.; Kang, Z.; Ji, W. Molecular mapping and marker development for the *Triticum dicoccoides*-derived stripe rust resistance gene *YrSM139-1B* in bread wheat cv. Shaanmai 139. *Theor. Appl. Genet.* **2015**, *129*, 369–376. [CrossRef]

23. Elkot, A.F.; Singh, R.; Kaur, S.; Kaur, J.; Chhuneja, P. Mapping novel sources of leaf rust and stripe rust resistance introgressed from *Triticum dicoccoides* in cultivated tetraploid wheat background. *J. Plant Biochem. Biotechnol.* **2020**, *30*, 336–342. [CrossRef]
24. Klymiuk, V.; Fatiukha, A.; Fahima, T. Wheat tandem kinases provide insights on disease-resistance gene flow and host–parasite co-evolution. *Plant J.* **2019**, *98*, 667–679. [CrossRef]
25. Gou, J.-Y.; Li, K.; Wu, K.; Wang, X.; Lin, H.; Cantu, D.; Uauy, C.; Dobon-Alonso, A.; Midorikawa, T.; Inoue, K.; et al. Wheat Stripe Rust Resistance Protein WKS1 Reduces the Ability of the Thylakoid-Associated Ascorbate Peroxidase to Detoxify Reactive Oxygen Species. *Plant Cell* **2015**, *27*, 1755–1770. [CrossRef] [PubMed]
26. Huang, L.; Sela, H.; Feng, L.; Chen, Q.; Krugman, T.; Yan, J.; Dubcovsky, J.; Fahima, T. Distribution and haplotype diversity of WKS resistance genes in wild emmer wheat natural populations. *Theor. Appl. Genet.* **2016**, *129*, 921–934. [CrossRef] [PubMed]
27. Santure, A.W.; Garant, D. Wild GWAS—association mapping in natural populations. *Mol. Ecol. Resour.* **2018**, *18*, 729–738. [CrossRef] [PubMed]
28. Sela, H.; Ezrati, S.; Ben-Yehuda, P.; Manisterski, J.; Akhunov, E.; Dvorak, J.; Breiman, A.; Korol, A. Linkage disequilibrium and association analysis of stripe rust resistance in wild emmer wheat (*Triticum turgidum* ssp. *dicoccoides*) population in Israel. *Theor. Appl. Genet.* **2014**, *127*, 2453–2463. [CrossRef]
29. Long, L.; Yao, F.; Yu, C.; Ye, X.; Cheng, Y.; Wang, Y.; Wu, Y.; Li, J.; Wang, J.; Jiang, Q.; et al. Genome-Wide Association Study for Adult-Plant Resistance to Stripe Rust in Chinese Wheat Landraces (*Triticum aestivum* L.) From the Yellow and Huai River Valleys. *Front. Plant Sci.* **2019**, *10*, 596. [CrossRef]
30. Yang, F.; Liu, J.; Guo, Y.; He, Z.; Rasheed, A.; Wu, L.; Cao, S.; Nan, H.; Xia, X. Genome-Wide Association Mapping of Adult-Plant Resistance to Stripe Rust in Common Wheat (*Triticum aestivum*). *Plant Dis.* **2020**, *104*, 2174–2180. [CrossRef]
31. Juliana, P.; Singh, R.P.; Singh, P.; Poland, J.A.; Bergstrom, G.C.; Huerta-Espino, J.; Bhavani, S.; Crossa, J.; Sorrells, M.E. Genome-wide association mapping for resistance to leaf rust, stripe rust and tan spot in wheat reveals potential candidate genes. *Theor. Appl. Genet.* **2018**, *131*, 1405–1422. [CrossRef]
32. Godoy, J.G.; Rynearson, S.; Chen, X.; Pumphrey, M. Genome-Wide Association Mapping of Loci for Resistance to Stripe Rust in North American Elite Spring Wheat Germplasm. *Phytopathology* **2018**, *108*, 234–245. [CrossRef]
33. Cheng, B.; Gao, X.; Cao, N.; Ding, Y.; Gao, Y.; Chen, T.; Xin, Z.; Zhang, L. Genome-wide association analysis of stripe rust-resistance loci in wheat accessions from southwestern China. *J. Appl. Genet.* **2020**, *61*, 37–50. [CrossRef]
34. Wang, J.; Zhang, Z. GAPIT Version 3: Boosting Power and Accuracy for Genomic Association and Prediction. *bioRxiv* **2020**, 403170. [CrossRef]
35. Zhang, Y.-W.; Tamba, C.L.; Wen, Y.-J.; Li, P.; Ren, W.-L.; Ni, Y.-L.; Gao, J.; Zhang, Y.-M. mrMLM v4.0.2: An R Platform for Multi-locus Genome-wide Association Studies. *Genom. Proteom. Bioinform.* **2020**, *18*, 481–487. [CrossRef] [PubMed]
36. Baranwal, D.; Cu, S.; Stangoulis, J.; Trethowan, R.; Bariana, H.; Bansal, U. Identification of genomic regions conferring rust resistance and enhanced mineral accumulation in a HarvestPlus Association Mapping Panel of wheat. *Theor. Appl. Genet.* **2022**, 1–18. [CrossRef] [PubMed]
37. Tomar, V.; Dhillon, G.S.; Singh, D.; Singh, R.P.; Poland, J.; Chaudhary, A.A.; Bhati, P.K.; Joshi, A.K.; Kumar, U. Evaluations of Genomic Prediction and Identification of New Loci for Resistance to Stripe Rust Disease in Wheat (*Triticum aestivum* L.). *Front. Genet.* **2021**, *12*, 710485. [CrossRef] [PubMed]
38. Liu, L.; Wang, M.; Zhang, Z.; See, D.R.; Chen, X. Identification of Stripe Rust Resistance Loci in U.S. Spring Wheat Cultivars and Breeding Lines Using Genome-Wide Association Mapping and *Yr* Gene Markers. *Plant Dis.* **2020**, *104*, 2181–2192. [CrossRef] [PubMed]
39. Habib, M.; Awan, F.S.; Sadia, B.; Zia, M.A. Genome-Wide Association Mapping for Stripe Rust Resistance in Pakistani Spring Wheat Genotypes. *Plants* **2020**, *9*, 1056. [CrossRef]
40. Gaurav, K.; Arora, S.; Silva, P.; Sánchez-Martín, J.; Horsnell, R.; Gao, L.; Brar, G.S.; Widrig, V.; Raupp, W.J.; Singh, N.; et al. Population genomic analysis of Aegilops tauschii identifies targets for bread wheat improvement. *Nat. Biotechnol.* **2021**, 1–10. [CrossRef]
41. Line, R.F.; Qayoum, A. *Virulence, Aggressiveness, Evolution, and Distribution of Races of Puccinia striiformis (the Cause of Stripe Rust of Wheat) in North America, 1968-87*; USDA-ARS: Washington, DC, USA, 1992.
42. Wan, A.; Wang, X.; Kang, Z.; Chen, X. Variability of the Stripe Rust Pathogen. In *Stripe Rust*; Springer: Berlin/Heidelberg, Germany, 2017; pp. 35–154.
43. Large, E.C. Growth Stages in Cereals Illustration of the Feekes Scale. *Plant Pathol.* **1954**, *3*, 128–129. [CrossRef]
44. Huang, S.; Steffenson, B.; Sela, H.; Stinebaugh, K. Resistance of *Aegilops longissima* to the Rusts of Wheat. *Plant Dis.* **2018**, *102*, 1124–1135. [CrossRef]
45. Chen, X. Epidemiology and control of stripe rust [*Puccinia striiformis* f. sp. *tritici*] on wheat. *Can. J. Plant Pathol.* **2005**, *27*, 314–337. [CrossRef]
46. Cheng, J.; Yan, J.; Sela, H.; Manisterski, J.; Lewinsohn, D.; Nevo, E.; Fahima, T. Pathogen race determines the type of resistance response in the stripe rust—*Triticum dicoccoides* pathosystem. *Physiol. Plant.* **2010**, *139*, 269–279. [CrossRef]
47. Poland, J.A.; Brown, P.J.; Sorrells, M.E.; Jannink, J.-L. Development of High-Density Genetic Maps for Barley and Wheat Using a Novel Two-Enzyme Genotyping-by-Sequencing Approach. *PLoS ONE* **2012**, *7*, e32253. [CrossRef]
48. Saintenac, C.; Jiang, D.; Wang, S.; Akhunov, E. Sequence-Based Mapping of the Polyploid Wheat Genome. *G3 Genes Genomes Genet.* **2013**, *3*, 1105–1114. [CrossRef] [PubMed]

49. Glaubitz, J.C.; Casstevens, T.M.; Lu, F.; Harriman, J.; Elshire, R.J.; Sun, Q.; Buckler, E.S. TASSEL-GBS: A High Capacity Genotyping by Sequencing Analysis Pipeline. *PLoS ONE* **2014**, *9*, e90346. [CrossRef] [PubMed]
50. Browning, B.L.; Zhou, Y.; Browning, S.R. A One-Penny Imputed Genome from Next-Generation Reference Panels. *Am. J. Hum. Genet.* **2018**, *103*, 338–348. [CrossRef]
51. Dowle, M.; Srinivasan, A.; Short, T.; Lianoglou, S. Data. Table: Extension of 'Data.Frame'. Available online: https://cran.r-project.org/web/packages/data.table/index.html (accessed on 25 February 2019).
52. Frutos, E.; Galindo, M.P.; Leiva, V. An interactive biplot implementation in R for modeling genotype-by-environment interaction. *Stoch. Environ. Res. Risk Assess.* **2014**, *28*, 1629–1641. [CrossRef]
53. Endelman, J.B. Ridge Regression and Other Kernels for Genomic Selection with R Package rrBLUP. *Plant Genome* **2011**, *4*, 250–255. [CrossRef]
54. Kruijer, W.; Boer, M.P.; Malosetti, M.; Flood, P.J.; Engel, B.; Kooke, R.; Keurentjes, J.J.; van Eeuwijk, F.A. Marker-based estimation of heritability in immortal populations. *Genetics* **2015**, *199*, 379–398. [CrossRef]
55. Stacklies, W.; Redestig, H.; Scholz, M.; Walther, D.; Selbig, J. pcaMethods a bioconductor package providing PCA methods for incomplete data. *Bioinformatics* **2007**, *23*, 1164–1167. [CrossRef]
56. Jombart, T. adegenet: A R package for the multivariate analysis of genetic markers. *Bioinformatics* **2008**, *24*, 1403–1405. [CrossRef]
57. Jombart, T.; Devillard, S.; Dufour, A.-B.; Pontier, D. Revealing cryptic spatial patterns in genetic variability by a new multivariate method. *Heredity* **2008**, *101*, 92–103. [CrossRef]
58. Therneau, T.M. Coxme: Mixed Effects Cox Models. Available online: https://cran.r-project.org/web/packages/coxme/index.html (accessed on 3 August 2020).
59. Bartoń, K. MuMIn: Multi-Model Inference. Available online: https://cran.r-project.org/web/packages/MuMIn/index.html (accessed on 4 May 2020).
60. Akaike, H. Information theory and an extension of the maximum likelihood principle. In *Selected papers of Hirotugu Akaike*; Springer: New York, NY, USA, 1998; pp. 199–213.
61. Benjamini, Y.; Hochberg, Y. Controlling the False Discovery Rate: A Practical and Powerful Approach to Multiple Testing. *J. R. Stat. Soc. Ser. B Methodol.* **1995**, *57*, 289–300. [CrossRef]
62. Basnet, B.R.; Ibrahim, A.M.H.; Chen, X.; Singh, R.P.; Mason, E.R.; Bowden, R.L.; Liu, S.; Hays, D.B.; Devkota, R.N.; Subramanian, N.K.; et al. Molecular Mapping of Stripe Rust Resistance in Hard Red Winter Wheat TAM 111 Adapted to the U.S. High Plains. *Crop Sci.* **2014**, *54*, 1361–1373. [CrossRef]
63. Suenaga, K.; Singh, R.P.; Huerta-Espino, J.; William, H.M. Microsatellite Markers for Genes *Lr34/Yr18* and Other Quantitative Trait Loci for Leaf Rust and Stripe Rust Resistance in Bread Wheat. *Phytopathology* **2003**, *93*, 881–890. [CrossRef] [PubMed]
64. Bulli, P.; Zhang, J.; Chao, S.; Chen, X.; Pumphrey, M. Genetic Architecture of Resistance to Stripe Rust in a Global Winter Wheat Germplasm Collection. *G3 Genes Genomes Genet.* **2016**, *6*, 2237–2253. [CrossRef]
65. Singh, R.; William, H.; Huerta-Espino, J.; Crosby, M. Identification and Mapping of Gene *Yr31* for Resistance to Stripe Rust in Triticum Aestivum Cultivar Pastor. In Proceedings of the 10th International Wheat Genetics Symposium, Paestum, Italy, 1–6 September 2003; Pogna, N.E., Romana, M., Pogna, E.A., Galterio, G., Eds.; Instituto Sperimentale per la Cerealicoltura: Rome, Italy, 2003; pp. 411–413.
66. Hou, L.; Ma, D.-F.; Hu, M.-L.; He, M.-M.; Lu, Y.; Jing, J.-X. Genetic Analysis and Molecular Mapping of an All-Stage Stripe Rust Resistance Gene in *Triticum aestivum-Haynaldia villosa* Translocation Line V3. *J. Integr. Agric.* **2013**, *12*, 2197–2208. [CrossRef]
67. Jimmy, J.L.; Babu, S. Role of OsWRKY transcription factors in rice disease resistance. *Trop. Plant Pathol.* **2015**, *40*, 355–361. [CrossRef]
68. Shindo, T.; Van Der Hoorn, R.A.L. Papain-like cysteine proteases: Key players at molecular battlefields employed by both plants and their invaders. *Mol. Plant Pathol.* **2007**, *9*, 119–125. [CrossRef]
69. Christopher, M.D.; Liu, S.; Hall, M.D.; Marshall, D.S.; Fountain, M.O.; Johnson, J.W.; Milus, E.A.; Garland-Campbell, K.A.; Chen, X.; Griffey, C.A. Identification and Mapping of Adult Plant Stripe Rust Resistance in Soft Red Winter Wheat VA00W-38. *Crop Sci.* **2013**, *53*, 871–879. [CrossRef]
70. Erayman, M.; Turktas, M.; Akdogan, G.; Gurkok, T.; Inal, B.; Ishakoglu, E.; Ilhan, E.; Unver, T. Transcriptome analysis of wheat inoculated with *Fusarium graminearum*. *Front. Plant Sci.* **2015**, *6*, 867. [CrossRef]
71. Figueiredo, L.; Santos, R.; Figueiredo, A. Defense and Offense Strategies: The Role of Aspartic Proteases in Plant–Pathogen Interactions. *Biology* **2021**, *10*, 75. [CrossRef]
72. Basnet, B.R.; Singh, R.P.; Ibrahim, A.M.H.; Herrera-Foessel, S.A.; Huerta-Espino, J.; Lan, C.; Rudd, J.C. Characterization of *Yr54* and other genes associated with adult plant resistance to yellow rust and leaf rust in common wheat Quaiu 3. *Mol. Breed.* **2013**, *33*, 385–399. [CrossRef]
73. Zhou, X.L.; Zhang, Y.; Zeng, Q.D.; Chen, X.M.; Han, D.J.; Huang, L.L.; Kang, Z.S. Identification of QTL for adult plant resistance to stripe rust in Chinese wheat landrace Caoxuan 5. *Euphytica* **2015**, *204*, 627–634. [CrossRef]
74. Lan, C.; Rosewarne, G.M.; Singh, R.P.; Herrera-Foessel, S.A.; Huerta-Espino, J.; Basnet, B.R.; Zhang, Y.; Yang, E. QTL characterization of resistance to leaf rust and stripe rust in the spring wheat line Francolin#1. *Mol. Breed.* **2014**, *34*, 789–803. [CrossRef]
75. Case, A.J.; Naruoka, Y.; Chen, X.; Garland-Campbell, K.; Zemetra, R.S.; Carter, A.H. Mapping Stripe Rust Resistance in a BrundageXCoda Winter Wheat Recombinant Inbred Line Population. *PLoS ONE* **2014**, *9*, e91758. [CrossRef]

76. Kumar, D. Salicylic acid signaling in disease resistance. *Plant Sci.* **2014**, *228*, 127–134. [CrossRef] [PubMed]
77. Yang, E.; Li, G.; Li, L.; Zhang, Z.; Yang, W.; Peng, Y.; Zhu, Y.; Yang, Z.; Rosewarne, G.M. Characterization of Stripe Rust Resistance Genes in the Wheat Cultivar Chuanmai45. *Int. J. Mol. Sci.* **2016**, *17*, 601. [CrossRef]
78. Pelgrom, A.J.E.; Meisrimler, C.-N.; Elberse, J.; Koorman, T.; Boxem, M.; van den Ackerveken, G. Host Targets of Effectors of the Lettuce Downy Mildew Bremia Lactucae from CDNA-Based Yeast Two-Hybrid Screening. *PLoS ONE* **2020**, *15*, e0226540. [CrossRef]
79. Lu, Y.; Wang, M.; Chen, X.; See, D.; Chao, S.; Jing, J. Mapping of *Yr62* and a small-effect QTL for high-temperature adult-plant resistance to stripe rust in spring wheat PI 192252. *Theor. Appl. Genet.* **2014**, *127*, 1449–1459. [CrossRef]
80. Chen, Y.; Li, Y.; Ren, H.; Zhou, J.; Wang, L.; Yang, Y.; Hao, X.; Wang, X. Genome-wide identification and expression profiling reveal the diverse role of Methyl-CpG-binding domain proteins in tea plant *Camellia sinensis*. *Beverage Plant Res.* **2021**, *1*, 10. [CrossRef]
81. Feng, J.; Zuo, L.L.; Zhang, Z.Y.; Lin, R.M.; Cao, Y.Y.; Xu, S.C. Quantitative trait loci for temperature-sensitive resistance to *Puccinia striiformis* f. sp. *tritici* in wheat cultivar Flinor. *Euphytica* **2010**, *178*, 321–329. [CrossRef]
82. Lu, Y.; Lan, C.; Liang, S.; Zhou, X.; Liu, D.; Zhou, G.; Lu, Q.; Jing, J.; Wang, M.; Xia, X.; et al. QTL mapping for adult-plant resistance to stripe rust in Italian common wheat cultivars Libellula and Strampelli. *Theor. Appl. Genet.* **2009**, *119*, 1349–1359. [CrossRef] [PubMed]
83. Mallard, S.; Gaudet, D.; Aldeia, A.; Abelard, C.; Besnard, A.L.; Sourdille, P.; Dedryver, F. Genetic analysis of durable resistance to yellow rust in bread wheat. *Theor. Appl. Genet.* **2005**, *110*, 1401–1409. [CrossRef] [PubMed]
84. Yuan, X.; Wang, H.; Cai, J.; Li, D.; Song, F. NAC transcription factors in plant immunity. *Phytopathol. Res.* **2019**, *1*, 3. [CrossRef]
85. Santra, D.K.; Chen, X.M.; Santra, M.; Campbell, K.G.; Kidwell, K.K. Identification and mapping QTL for high-temperature adult-plant resistance to stripe rust in winter wheat (*Triticum aestivum* L.) cultivar 'Stephens'. *Theor. Appl. Genet.* **2008**, *117*, 793–802. [CrossRef]
86. Bariana, H.S.; Bansal, U.; Schmidt, A.; Lehmensiek, A.; Kaur, J.; Miah, H.; Howes, N.; McIntyre, C. Molecular mapping of adult plant stripe rust resistance in wheat and identification of pyramided QTL genotypes. *Euphytica* **2010**, *176*, 251–260. [CrossRef]
87. Steele, J.F.C.; Hughes, R.K.; Banfield, M.J. Structural and biochemical studies of an NB-ARC domain from a plant NLR immune receptor. *PLoS ONE* **2019**, *14*, e0221226. [CrossRef] [PubMed]
88. Zhao, X.-Y.; Qi, C.-H.; Jiang, H.; Zheng, P.-F.; Zhong, M.-S.; Zhao, Q.; You, C.-X.; Li, Y.-Y.; Hao, Y.-J. Functional identification of apple on MdHIR4 in biotic stress. *Plant Sci.* **2019**, *283*, 396–406. [CrossRef] [PubMed]
89. Liu, J.; He, Z.; Wu, L.; Bai, B.; Wen, W.; Xie, C.; Xia, X. Genome-Wide Linkage Mapping of QTL for Adult-Plant Resistance to Stripe Rust in a Chinese Wheat Population Linmai x Zhong 892. *PloS ONE* **2015**, *10*, e0145462. [CrossRef]
90. Liu, X.; Song, L.; Zhang, H.; Lin, Y.; Shen, X.; Guo, J.; Su, M.; Shi, G.; Wang, Z.; Lu, G. Rice ubiquitin-conjugating enzyme OsUBC26 is essential for immunity to the blast fungus *Magnaporthe oryzae*. *Mol. Plant Pathol.* **2021**, *22*, 1613–1623. [CrossRef]
91. Douchkov, D.; Lueck, S.; Hensel, G.; Kumlehn, J.; Rajaraman, J.; Johrde, A.; Doblin, M.S.; Beahan, C.T.; Kopischke, M.; Fuchs, R.; et al. The barley (*Hordeum vulgare*) cellulose synthase-like D2 gene (HvCslD2) mediates penetration resistance to host-adapted and nonhost isolates of the powdery mildew fungus. *New Phytol.* **2016**, *212*, 421–433. [CrossRef]
92. Sela, H.; Loutre, C.; Keller, B.; Schulman, A.; Nevo, E.; Korol, A.; Fahima, T. Rapid linkage disequilibrium decay in the *Lr10* gene in wild emmer wheat (*Triticum dicoccoides*) populations. *Theor. Appl. Genet.* **2010**, *122*, 175–187. [CrossRef] [PubMed]
93. Morrell, P.; Toleno, D.M.; Lundy, K.E.; Clegg, M.T. Low levels of linkage disequilibrium in wild barley (*Hordeum vulgare* ssp. *spontaneum*) despite high rates of self-fertilization. *Proc. Natl. Acad. Sci. USA* **2005**, *102*, 2442–2447. [CrossRef] [PubMed]
94. Nordborg, M.; Borevitz, J.; Bergelson, J.; Berry, C.C.; Chory, J.; Hagenblad, J.; Kreitman, M.; Maloof, J.; Noyes, T.; Oefner, P.J.; et al. The extent of linkage disequilibrium in *Arabidopsis thaliana*. *Nat. Genet.* **2002**, *30*, 190–193. [CrossRef]
95. Chao, S.; Dubcovsky, J.; Dvorak, J.; Luo, M.-C.; Baenziger, S.P.; Matnyazov, R.; Clark, D.R.; Talbert, L.E.; Anderson, J.A.; Dreisigacker, S.; et al. Population- and genome-specific patterns of linkage disequilibrium and SNP variation in spring and winter wheat (*Triticum aestivum* L.). *BMC Genom.* **2010**, *11*, 727. [CrossRef] [PubMed]
96. GRIN-Global. Available online: https://npgsweb.ars-grin.gov/gringlobal/search (accessed on 8 December 2021).
97. GRIS. Available online: http://www.wheatpedigree.net/ (accessed on 8 December 2021).
98. Xiang, C.; Feng, J.Y.; Wang, M.N.; Chen, X.M.; See, D.R.; Wan, A.M.; Wang, T. Molecular Mapping of Stripe Rust Resistance Gene *Yr76* in Winter Club Wheat Cultivar Tyee. *Phytopathology* **2016**, *106*, 1186–1193. [CrossRef] [PubMed]
99. Lillemo, M.; Asalf, B.; Singh, R.; Huerta-Espino, J.; Chen, X.; He, Z.; Bjørnstad, Å. The Adult Plant Rust Resistance Loci Lr34/*Yr18* and *Lr46/Yr29* Are Important Determinants of Partial Resistance to Powdery Mildew in Bread Wheat Line Saar. *Theor. Appl. Genet.* **2008**, *116*, 1155–1166. [CrossRef] [PubMed]
100. Dmochowska-Boguta, M.; Kloc, Y.; Zielezinski, A.; Werecki, P.; Nadolska-Orczyk, A.; Karlowski, W.M.; Orczyk, W. TaWAK6 encoding wall-associated kinase is involved in wheat resistance to leaf rust similar to adult plant resistance. *PLoS ONE* **2020**, *15*, e0227713. [CrossRef]
101. Ensembl Genomes *Triticum_dicoccoides*. Available online: http://plants.ensembl.org/Triticum_dicoccoides/Info/Index (accessed on 8 December 2021).